Measurement of the $^2H(\gamma,\pi^0)$ reaction near threshold

J. C. Bergstrom,* R. Igarashi, J. M. Vogt, N. Kolb, R. E. Pywell, and D. M. Skopik
Saskatchewan Accelerator Laboratory, University of Saskatchewan, Saskatoon, Saskatchewan, Canada S7N 5C6

E. Korkmaz
Physics Department, University of Northern British Columbia, Prince George, British Columbia, Canada V2N 4Z9

(Received 3 December 1997)

Total and differential cross sections for the reaction $^2H(\gamma,\pi^0)$ have been investigated within 20 MeV of threshold using the tagged photon facility at SAL in conjunction with the π^0 spectrometer IGLOO. The differential measurements are the first to be reported in the threshold region, while the total cross section is a significant improvement over the only previous measurement. We give the first determination of the electric dipole amplitude for π^0 photoproduction from the deuteron in the threshold region. The threshold amplitude (E_d) has recently been calculated within the framework of chiral perturbation theory (ChPT). The present result for E_d falls about 20% below the ChPT value. We confirm the predicted sign (negative). Above threshold we find no evidence for a unitarity cusp such as is observed in the dipole amplitude for $^1H(\gamma,\pi^0)$. Finally, the elementary P-wave amplitude $P_1^{(+)}$ as deduced from the angular distributions is compared with ChPT predictions. A substantial discrepancy with theory is evident, perhaps a signal of two-body effects. [S0556-2813(98)03306-8]

PACS number(s): 25.20.Lj, 13.60.Le

I. INTRODUCTION

The total and differential cross sections for the reaction $^2H(\gamma,\pi^0)$ have been measured within 20 MeV of threshold at SAL (Saskatchewan Accelerator Laboratory) using tagged photons and the large acceptance π^0 spectrometer IGLOO. This represents the first comprehensive investigation of π^0 photoproduction from the deuteron in the threshold region. The literature reports only one previous investigation at low energy, and this was confined to a measurement of the total cross section within 10 MeV of threshold [1]. The results were presented in the form of an error band and are of limited statistical quality. No previous angular distribution measurements exist in the low energy domain.

One focus of our study concerns the effective S-wave photoproduction amplitude for the *elastic* process $^2H(\gamma,\pi^0)^2H$, both at threshold and above threshold. Since the *inelastic* reaction $^2H(\gamma,\pi^0)np$ also contributes and is unresolved in the measurements, the relative contribution of this channel has been estimated by a theoretical model, a variation of which gives a good description of the related $^2H(\gamma,\pi^+)nn$ reaction. We estimate that the inelastic channel contributes about 16% of the total experimental $^2H(\gamma,\pi^0)$ cross section at our highest energy and rapidly decreases in relative strength with decreasing energy.

Let us review some of the general issues pertinent to the $^2H(\gamma,\pi^0)^2H$ reaction at low energies. In the impulse approximation it is sufficient to consider only the isovector-even S- and P-wave pion-nucleon (πN) photoproduction amplitudes, higher partial waves being negligible. The S-wave electric dipole amplitude is denoted by $E_{0+}^{(+)}$ and is defined in terms of the individual nucleon amplitudes by

$$E_{0+}^{(+)}=\frac{1}{2}\left[E_{0+}(\pi^0 p)+E_{0+}(\pi^0 n)\right]. \tag{1}$$

The P-wave πN amplitudes are denoted by $P_{1,2,3}^{(+)}$ and are defined in terms of the usual multipole amplitudes by

$$P_1^{(+)}=3E_{1+}^{(+)}+M_{1+}^{(+)}-M_{1-}^{(+)},$$

$$P_2^{(+)}=3E_{1+}^{(+)}-M_{1+}^{(+)}+M_{1-}^{(+)},$$

$$P_3^{(+)}=2M_{1+}^{(+)}+M_{1-}^{(+)}. \tag{2}$$

The individual amplitudes $P_{2,3}^{(+)}$ are unimportant here since they occur as a particular combination in the cross sections and cannot be separated in the absence of polarized degrees of freedom. The amplitude $P_1^{(+)}$, however, is distinguished since, together with $E_{0+}^{(+)}$, it drives the forward-backward asymmetry in the differential cross section.

Application of the free amplitudes to an extended nuclear system such as the deuteron immediately leads to several complications. For example, the spatial extent of the deuteron (as represented by its form factor) in effect induces higher partial waves as viewed from the pion-nuclear (πA) frame. *Thus analysis of the data solely in terms of S and P waves in the πA frame will not suffice*. At the theoretical level it is necessary to transform the fundamental amplitudes from the πN frame to the πA frame, and this together with the attendant Fermi motion tends to obscure the free nucleon amplitudes.

Nevertheless, to a certain degree of approximation one can accommodate the preceding in a simple formalism that still reflects the underlying πN amplitudes. This formalism is developed in Appendix A and will be employed in our

*Electronic address: bergstrom@skatter.usask.ca

analysis of the effective S-wave amplitude above threshold and in addition will permit us to comment on the P-wave amplitude $P_1^{(+)}$.

A few of the more specific issues relevant to the present study are outlined as follows.

(1) As demonstrated through recent measurements of the $p(\gamma,\pi^0)$ reaction near threshold [2,3], the S-wave amplitude $E_{0+}(\pi^0 p)$ displays a remarkable energy dependence. Between the π^0 and π^+ thresholds (about 6 MeV), the amplitude decreases from -1.3 to -0.5 (in units of $10^{-3}/m_{\pi^+}$), after which it recovers to -1.1 about 20 MeV above the π^0 threshold. This behavior is interpreted as a ''unitarity cusp'' deriving from isospin breakdown that splits the neutral and charged pion masses [3,4]. A similar cusp should be evident in the neutron amplitude $E_{0+}(\pi^0 n)$, and indeed the sign of the modulating term driving the cusp must be identical for the proton and neutron as can be argued from elementary considerations. Thus the amplitude $E_{0+}^{(+)}$ of Eq. (1) should display a substantial modulation since the individual nucleon cusps combine constructively. Yet as will be seen, we find no evidence for a cusp in the deuteron dipole amplitude.

(2) The unitarity cusp is driven by a one-nucleon rescattering process, wherein πN charge exchange on the target nucleon leads to the final neutral pion. In the deuteron a two-nucleon rescattering process can also occur, wherein a charged pion is photoproduced on one nucleon and subsequently undergoes πN charge exchange on the second (spectator) nucleon. Koch and Woloshyn [5] pioneered the calculation of this process and concluded that it should totally dominate over the elementary $^2\mathrm{H}(\gamma,\pi^0)^2\mathrm{H}$ mechanism. There has been debate in the literature over this conclusion. For example, Blaazer *et al.* [6] employed a Faddeev technique and contend that the one-nucleon rescattering should dominate over the two-nucleon process. Recently, the question has been addressed by Beane *et al.* [7] using the formalism of chiral perturbation theory (ChPT), and the two-nucleon rescattering was found to be very large, sufficient in fact to change the sign of the effective S-wave amplitude at threshold from a positive quantity to a negative one. It is important to note here that the ChPT version of $E_{0+}^{(+)}$ as defined by Eq. (1) is numerically positive, in marked contrast to the negative amplitude predicted by the pre-ChPT low energy theorems (LET's) and employed by all other authors in their calculations of $^2\mathrm{H}(\gamma,\pi^0)$. The threshold amplitudes of Beane *et al.* are

$$E_{0+}(\pi^0 p) = -1.16,$$

$$E_{0+}(\pi^0 n) = +2.13, \tag{3}$$

in the usual units of $10^{-3}/m_{\pi^+}$. The proton amplitude is in reasonable agreement with the experimental value $E_{0+}(\pi^0 p) = -1.3 \pm 0.08$ [2,3]. The amplitudes of Eq. (3) include the ChPT equivalent of one-nucleon rescattering. Interestingly, in the absence of two-nucleon rescattering, the ChPT amplitude $E_{0+}^{(+)}$ extrapolated slightly above threshold produces a forward-peaked pion angular distribution. Inclusion of the two-nucleon rescattering causes it to be backward peaked. Our results clearly demonstrate that the cross section is indeed backward peaked.

(3) Above threshold, the two-nucleon rescattering process introduces an angular dependence into the effective S-wave amplitude. To see how this arises, let us first consider the situation at π^0 threshold. At threshold the reduced cross section may be expressed as [7]

$$\left.\frac{k}{q}\frac{d\sigma}{d\Omega}\right|_{q=0} = \frac{8}{3}E_d^2, \tag{4}$$

where E_d is the threshold dipole amplitude for the deuteron and k and q are, respectively, the photon and pion momenta in the πA frame. The dipole amplitude may be further decomposed,

$$E_d = \left(1 - \frac{3}{2}P_D\right)\eta F(k)\overline{E}^{(+)}, \tag{5}$$

where $P_D \approx 0.06$ is the D-state probability, $\eta \approx 1.07$ is a frame-transformation factor defined in Appendix A, $F(k)$ is the deuteron form factor evaluated at threshold, and $\overline{E}^{(+)}$ is the quantity referred to herein as the ''effective'' S-wave amplitude. The assumptions underlying Eq. (5) are described in Appendix A. In the absence of two-nucleon rescattering (and ignoring the P-wave modification to $\overline{E}^{(+)}$ induced by Fermi motion), we have the obvious relation

$$F(k)\overline{E}^{(+)} = F(k)E_{0+}^{(+)}, \tag{6}$$

where $E_{0+}^{(+)}$ is defined by Eq. (1). In the presence of rescattering we replace Eq. (6) by

$$F(k)\overline{E}^{(+)} = F(k)[E_{0+}^{(+)} + \Delta E], \tag{7}$$

where

$$\Delta E = -\frac{\eta}{2}[E_{0+}(\pi^+ n) - E_{0+}(\pi^- p)]a_{\mathrm{cx}}\frac{1}{F(k)}\left\langle \frac{1}{r}e^{i\vec{k}\cdot\vec{r}/2}\right\rangle. \tag{8}$$

Here $a_{\mathrm{cx}} = \sqrt{2}(a_1 - a_3)/3$ is the $\pi^+ n \to \pi^0 p$ charge exchange amplitude, while the expectation value is evaluated between deuteron states. The rescattering correction as expressed by Eq. (8) is a convenient approximation, but ignores Fermi motion, which may play an important role. For an introduction to the derivation of ΔE, we refer to the book by Ericson and Weise [8].

The effective S-wave amplitude at threshold is now defined by

$$\overline{E}^{(+)} = E_{0+}^{(+)} + \Delta E. \tag{9}$$

In the region *above* threshold Eq. (8) is modified due to the finite pion momentum $\vec{q}$. For example, we replace $\vec{k} \to \vec{k} + \vec{q}$ in the expectation value and $F(k) \to F(Q)$ in the denominator, where $\vec{Q} = \vec{k} - \vec{q}$ is the angular-dependent momentum transfer. [The full expression is presented in Appendix C, Eq. (C5).] Therefore, through the correction ΔE, the effective amplitude $\overline{E}^{(+)}$ now becomes a function of angle, the dependence being largely driven by the form factor in the denominator of Eq. (8).

It is impossible to quantify the angular dependence of $\overline{E}^{(+)}$ solely from the experimental angular distributions since there are other degrees of freedom in our model cross section which can imitate the angular dependence. Nevertheless, as part of our investigation we will also consider an angular dependence for $\overline{E}^{(+)}$ in proportion to $1/F(Q)$. The effect is minimal, except to reduce the extracted P-wave amplitude $P_1^{(+)}$ and move it closer to the free-nucleon ChPT prediction [7,11].

(4) The ChPT calculations [7] provide the first definitive prediction for the threshold dipole amplitude E_d, namely,

$$E_d=(-1.8\pm0.2)\times10^{-3}/m_{\pi^+}. \tag{10}$$

Stripping away the nuclear factors using Eq. (5) gives the effective S-wave amplitude at threshold,

$$\overline{E}_{\rm th}^{(+)}=(-2.3\pm0.3)\times10^{-3}/m_{\pi^+}. \tag{11}$$

A major contribution to this amplitude arises from three-body corrections (roughly, our two-nucleon rescattering), sufficient in fact to flip the sign of $\overline{E}_{\rm th}^{(+)}$ as previously noted. The present measurements confirm the prediction as to sign. As to magnitude, extrapolation of the (reduced) total cross section to threshold yields an amplitude about 20% smaller than Eq. (10).

(5) The neutron amplitude $E_{0+}(\pi^0 n)$ cannot be deduced from the deuteron cross sections without a reliable estimate of the two-nucleon rescattering contribution to the effective S-wave amplitude. Although at present we are still unable to make a quantitative statement concerning the neutron amplitude, we are able to make a qualitative statement. Specifically, we will demonstrate that the threshold amplitude E_d (or $\overline{E}^{(+)}$) as derived from the data is more compatible with the ChPT neutron amplitude of Eq. (3) than with the LET value $E_{0+}(\pi^0 n)=+0.5$. The striking incongruity between the ChPT and LET predictions for the neutron amplitude arises in part from the contribution of the so-called ''triangle diagram,'' where the photon connects to a virtual in-flight charged pion and which diagram is excluded from the classical LET's. The $p(\gamma,\pi^0)$ experiments [2,3] seem to have resolved the issue in the proton sector in favor of the ChPT prediction. The present results point to a similar but tentative conclusion in the neutron sector.

Theoretical predictions of the $^2H(\gamma,\pi^0)^2H$ cross section in the region 0–10 MeV above threshold differ markedly in their conclusions [5,6,9,10]. There is general agreement that the angular distributions should be backward peaked, but this automatically follows from the LET value for $E_{0+}^{(+)}$ employed in these calculations. The main point of disagreement between the various estimates appears to lie in the two-nucleon rescattering contribution ΔE. For example, Bosted and Laget [9], using Reid soft-core wave functions, calculate a much smaller contribution than Koch and Woloshyn [5] who employed Hulthén wave functions, and the respective (reduced) cross sections accordingly differ markedly near threshold. The recent calculation by Kamalov *et al.* [10] explores the variation of $E_{0+}^{(+)}$ as it effects the total and differential cross sections 8 MeV above threshold. However, as with the other calculations, the total cross section near threshold is somewhat larger than the present experimental findings.

The angular dependence of the differential cross section is very sensitive to the P-wave amplitudes $P_{1,2,3}^{(+)}$ as defined by Eq. (2), and $P_1^{(+)}$ in particular drives the forward-backward asymmetry. Contrary to the predictions of Refs. [9,10], we observe significant strength in the forward direction for energies about 8 MeV above threshold. These models share a common reliance on the well-known Blomqvist-Laget (BL) amplitude, and a comparison between the BL predictions of $P_{1,2,3}^{(+)}$ at low energy and the rather successful ChPT predictions [11] might shed some light on the forward discrepancy.

This paper is organized as follows. Experimental details are described in Sec. II. In Sec. III we present the total cross section and deduce the electric dipole amplitude at threshold by extrapolation. The pion angular distributions are given in Sec. IV and are analyzed within a theoretical framework to yield the electric dipole amplitude as a function of energy. A discussion of our findings is given in Sec. V, and concluding remarks are summarized in Sec. VI. In Appendixes A and B we outline our models for the elastic and inelastic cross sections used in the data analyses. Finally, in Appendix C we provide a brief discussion of the imaginary part of the electric dipole amplitude.

II. EXPERIMENTAL DETAILS

This experiment was performed at SAL using the tagged photon facility [12] in conjunction with the π^0 spectrometer IGLOO [13]. Bremsstrahlung was generated by a 206.2 MeV electron beam with an energy spread of about 50 keV and a duty factor of 60–70 % as provided by the pulse-stretcher ring EROS. The photon tagger was equipped with a 62-channel medium-resolution detector array that permitted measurements over an excitation region of 20 MeV using a single setting of the tagging spectrometer. Each channel of the array spanned about 500 keV in tagged photon energy.

The π^0 spectrometer IGLOO is described in detail in Ref. [13]. Basically, it consists of a rectangular box of 68 lead glass detectors symmetrically arranged to define a hollow cave of dimensions $100\times40\times40$ cm^3, and in this ''closed'' configuration it is employed exclusively for total cross section measurements, exploiting the large geometric acceptance. The efficiency for π^0 detection is about 83% near threshold, decreasing to about 74% at the maximum energy, and is relatively insensitive to the pion angular distribution. The absolute response of the spectrometer has been extensively modeled by Monte Carlo simulations, which have been substantiated by measurements of the $^{12}C(\gamma,\pi^0)$ reaction [13,14] through comparison with the world database.

For pion angular distribution measurements, IGLOO is split along a diagonal of the cave and each L-shaped arm is retracted about 42 cm in order to enhance the angular resolution to the π^0-decay photons. In this ''open'' mode, pion detection efficiency is reduced to about 28% near threshold. Pion emission angles are reconstructed from the respective photon angles and energies using the reconstruction algorithm described in [13].

Pions are identified from their characteristic decay into two photons as observed by IGLOO in coincidence with the

photon tagging spectrometer. There are two sources of background to contend with. One is due to untagged pions created by photons beyond the tagging range and in accidental coincidence with the photon tagger. The other source of background is e^+e^- pair production, followed by large angle rescattering, thus mimicking π^0 decay photons. Since the spectrometer does not employ charged-particle veto counters for reasons discussed in [13], the e^+e^- background has to be rejected by software.

Some of the background events are rejected through cuts on the individual apparent decay photon energies. However, a much more effective cut is based on the angular correlation between the two π^0 decay photons, which, especially near threshold, is very different from the forward-peaked e^+e^- background. This cut is most effective in the region where it is most needed, i.e., where the true photopion cross section is smallest. As described in [13], illegal pairs are masked out by comparing the detector patterns against an extensive set of Monte Carlo generated patterns that encompass nearly all legal π^0 events.

The remaining background consists of untagged neutral pions and e^+e^- pairs, and a small quantity of tagged e^+e^- events. The untagged background contribution is estimated from TDC (time-to-digital converter) spectra that measure the timing correlation between IGLOO and tagged photons. The remaining tagged e^+e^- background is deduced by comparing masked data against unmasked data, as discussed in [13].

The target consisted of liquid deuterium contained within a cylindrical Mylar cell 10.8 cm long and 8.5 cm in diameter situated in the center of the π^0 spectrometer. The effective target thickness was determined *in situ* to an accuracy of $\pm 0.6\%$ by measuring the forward pair production relative to a calibrated aluminum target, utilizing the well-known atomic cross sections. Data were also accumulated on the reaction $^{12}\mathrm{C}(\gamma,\pi^0)$ as a continuity check of the IGLOO response against previous $^{12}\mathrm{C}(\gamma,\pi^0)$ measurements at SAL.

The photon tagging efficiency was about 70% and was repeatedly measured throughout the run using a lead-glass detector.

III. TOTAL CROSS SECTION AND EXTRAPOLATION TO THRESHOLD

The total cross section σ within about 20 MeV of threshold ($E_{\mathrm{th}}=139.8$ MeV), including the unresolved inelastic contribution from $^2\mathrm{H}(\gamma,\pi^0)np$, is shown in Fig. 1. The errors in σ reflect the counting statistics, uncertainties in the measured photon tagging efficiencies, and background subtractions, but do not reflect the overall systematic error estimated to be about 4%. The data points in the figure correspond to the individual channels of the tagging spectrometer detector array.

The *reduced* cross section $(k/q)\sigma$ is displayed in Fig. 2. Here k and q are the photon and pion momenta in the c.m. frame, with q evaluated for the elastic channel $^2\mathrm{H}(\gamma,\pi^0)^2\mathrm{H}$. The square point at threshold derives from the ChPT prediction [7] for the dipole amplitude E_d [Eq. (10)].

The solid curve in Fig. 2 is our theoretical estimate for the reduced inelastic cross section $^2\mathrm{H}(\gamma,\pi^0)np$, described in detail in Appendix B. The inelastic threshold is 142.2 MeV.

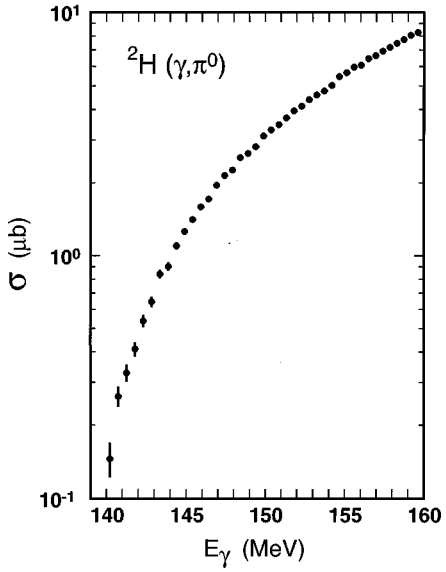

FIG. 1. Total cross section for $^2\mathrm{H}(\gamma,\pi^0)$ in the threshold region as a function of photon energy. These results include the unresolved contribution from the inelastic process $^2\mathrm{H}(\gamma,\pi^0)np$. The elastic threshold is 139.8 MeV, and the inelastic threshold is 142.2 MeV.

A theoretical uncertainty of roughly $\pm 25\%$ is ascribed to this cross section based on an error analysis of the model parameters. The elastic value for q is used in defining the reduced cross section since the pion momentum is not unique in the breakup channel. The inelastic cross section rises quickly with energy as dictated by elementary phase-space considerations and contributes about 16% to the total experimental cross section at maximum energy.

The dipole amplitude E_d is deduced by extrapolating the reduced cross section to threshold and employing the identity Eq. (4). To this purpose the reduced cross section is fit by least squares to a polynomial in $(E-E_{\mathrm{th}})$ where E_{th} is the

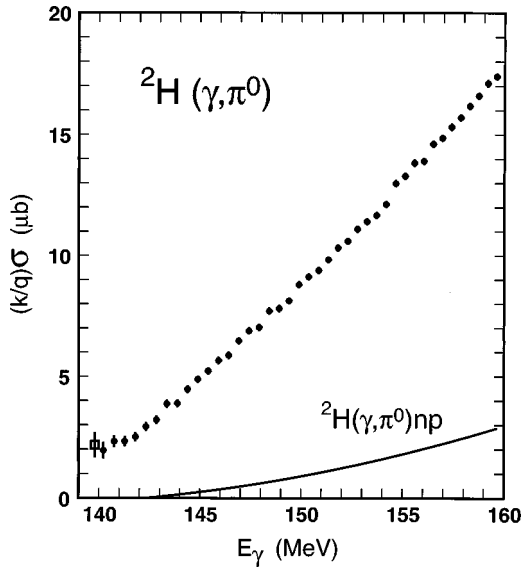

FIG. 2. Reduced total cross section for $^2\mathrm{H}(\gamma,\pi^0)$. The square point at threshold (139.8 MeV) is the prediction from chiral perturbation theory [7]. The curve is the theoretical estimate for the inelastic reaction $^2\mathrm{H}(\gamma,\pi^0)np$ described in Appendix B. An uncertainty of roughly $\pm 25\%$ is assigned to this estimate.

TABLE I. Dipole amplitude E_d as deduced by extrapolating the reduced cross section $(k/q)\sigma$ to threshold under various scenarios. The maximum order of the polynomial in $(E-E_{\rm th})$ is represented by n. The quality of the fit is indicated by the chi square per degree of freedom, χ^2_ν. The error assigned to the final estimate for E_d includes statistical and systematic uncertainties.

	n	χ^2_ν	$E_d(10^{-3}/m_\pi)$
Inelastic contribution removed			
All data (0–20 MeV)	2	1.3	-1.49 ± 0.04
Half data (0–10 MeV)	2	1.2	-1.47 ± 0.06
	1	1.2	-1.42 ± 0.04
Inelastic contribution not removed			
All data (0–20 MeV)	2	1.4	-1.43 ± 0.04
Half data (0–10 MeV)	2	1.4	-1.43 ± 0.06
	1	1.7	-1.26 ± 0.04
Final estimate			-1.45 ± 0.09

threshold energy. The maximum order of the polynomial is determined by application of the ''F test'' of an additional term in a finite polynomial representation of a fitting function [15]. The experimental data portrayed in Fig. 2 clearly demonstrate a nonlinear dependence, but this is largely due to the inelastic contribution. Removal of the latter yields a residual (presumably elastic) reduced cross section which is almost linear in energy, and indeed the F test as applied to the residual cross section indicates that terms of third order and higher in $(E-E_{\rm th})$ are redundant.

The threshold amplitude E_d is summarized in Table I under various analysis scenarios. These scenarios encompass the complete data set (0–20 MeV), half the data set (0–10 MeV), and a linear fit. Although we assign an uncertainty of 25% to the inelastic contribution, ignoring this component completely is seen to have only a modest influence on the extrapolation to threshold. All things considered, we conclude

$$E_d=(-1.45\pm0.09)\times10^{-3}/m_\pi, \tag{12}$$

which is about 20% lower than the ChPT prediction, Eq. (10). The effective S-wave amplitude from Eq. (5) is

$$\overline{E}^{(+)}_{\rm th}=(-1.89\pm0.12)\times10^{-3}/m_\pi, \tag{13}$$

to be compared with Eq. (11). The corresponding reduced cross section at threshold is 1.41 ± 0.18 μb. The signs of the above amplitudes anticipate the analysis of the pion angular distributions, described in the following section.

The discrepancy between Eq. (12) and the ChPT prediction, although not excessive, deserves some comment. The underlying effective S-wave amplitude is expressed by $\overline{E}^{(+)}=E^{(+)}_{0+}+\Delta E$, where $E^{(+)}_{0+}$ is defined by Eq. (1) and ΔE is the two-nucleon rescattering correction (or ChPT equivalent). It is very unlikely that the source of the discrepancy resides in $E^{(+)}_{0+}$ since this would require a neutron amplitude $E_{0+}(\pi^0 n)$ in considerable excess of the ChPT prediction of Eq. (3). However, if we adopt the predictions of Eq. (3), then a slight downward renormalization of ΔE,

$$\Delta E\approx0.8\Delta E_{\rm ChPT}, \tag{14}$$

brings theory and experiment into alignment.

We are not in a position to extract the neutron amplitude $E_{0+}(\pi^0 n)$ given the theoretical uncertainty in ΔE. However, we can differentiate between the ChPT values for the nucleon amplitudes and the ''old'' LET predictions. The former leads to the modest renormalization expressed by Eq. (14). The latter would imply a rescattering correction $\Delta E\approx0.4\Delta E_{\rm ChPT}$. On the other hand, if we adopt the experimental proton amplitude $[E_{0+}(\pi^0 p)=-1.3]$ and maintain the LET neutron amplitude $[E_{0+}(\pi^0 n)=+0.5]$, then $\Delta E\approx0.5\Delta E_{\rm ChPT}$. In either case, these renormalizations would imply a serious deficiency in the current theoretical estimate of the rescattering correction. *If one accepts the prediction of ΔE within $\pm25\%$ or so, then the experimental value of E_d definitely favors the ChPT prediction for the neutron amplitude given by Eq. (3).*

An additional correction to $\overline{E}^{(+)}$, which we denote as ΔE_p, arises from the $\pi N\rightarrow\pi A$ frame transformation of the elementary P-wave amplitudes and is closely associated with the Fermi motion. The authors of Ref. [7] conclude that this additional correction is negligible. Our estimates suggest otherwise, and we find $\Delta E_p\approx-0.3\times10^{-3}/m_\pi$ [see Appendix A, Eqs. (A14) and (A15)]. This unresolved discrepancy may reflect on the above discussion.

We conclude the present discussion with a comment concerning the extrapolation procedure described above. The analysis assumes a monotonic and smoothly increasing total cross section as a function of photon energy. In principle this assumption could be compromised if, for example, the effective S-wave amplitude $\overline{E}^{(+)}$ exhibits a strong cusp as in the free-proton case [2,3]. However, analysis of the pion angular distributions described below fails to reveal any cusplike behavior of significance.

IV. PION ANGULAR DISTRIBUTIONS

A. Preamble

The pion angular distributions in the c.m. frame are shown in Fig. 3. Each is based on a grouping of four detector channels of the photon tagging spectrometer and subtends about 2 MeV of excitation. The distributions display a strong angular asymmetry at low energy, which tends to weaken with increasing energy. This behavior is attributed to a gradual increase in the πN P-wave strength against a relatively stable S-wave contribution as will be demonstrated. Included in Fig. 3 are theoretical estimates for the inelastic cross section $^2H(\gamma,\pi^0)np$, as described in Appendix B.

Our aim here is to deduce the effective amplitude $\overline{E}^{(+)}$ as a function of energy from the pion angular distributions. Clearly, some sort of parametrization of the differential cross section is necessary, and for this purpose we will employ the model cross section described in detail in Appendix A. The model is derived in the plane-wave impulse approximation (PWIA) and is given by Eq. (A22):

$$\frac{k}{q}\frac{d\sigma}{d\Omega}=F^2(Q)\left\{\left(1-\frac{3}{2}P_D\right)^2\left[\frac{8}{3}(\eta\overline{E}^{(+)}+P_1^{(+)}\cos\theta)^2+\frac{4}{3}(P_2^{(+)}\sin\theta)^2\right]+2(P_3^{(+)}\sin\theta)^2\right\}, \tag{15}$$

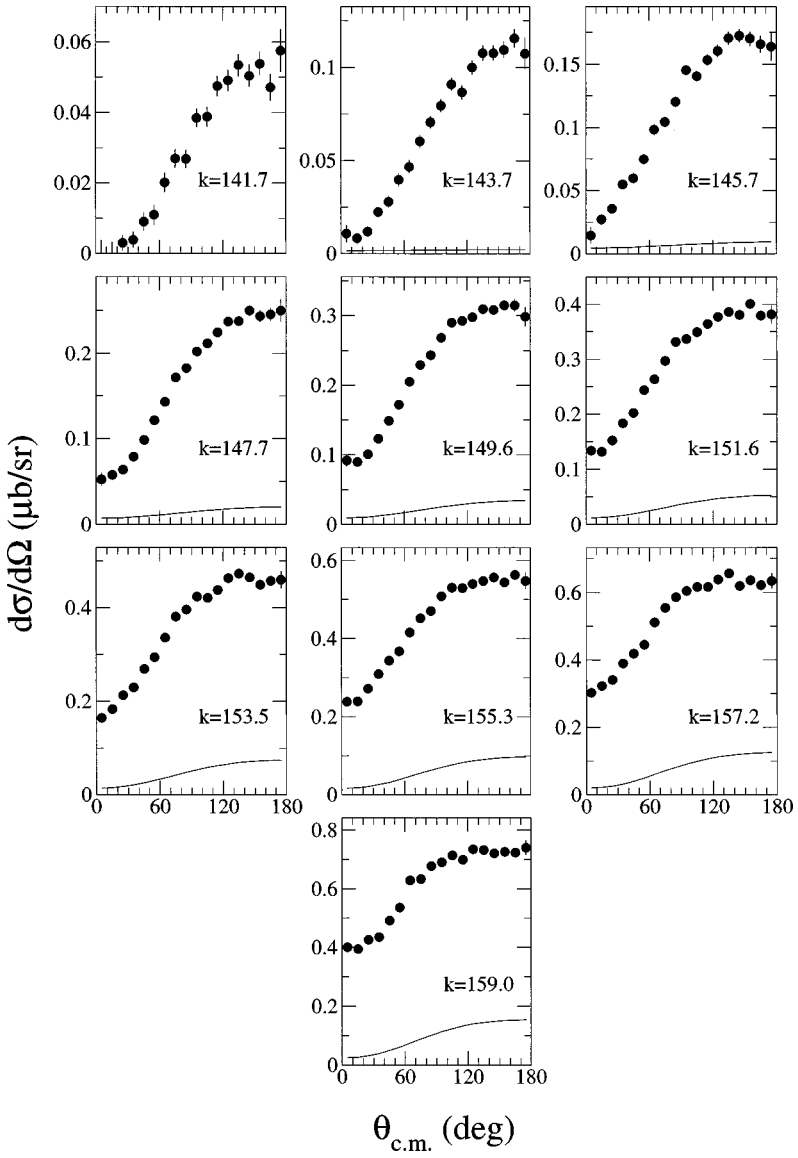

FIG. 3. Pion angular distributions for $^2\mathrm{H}(\gamma,\pi^0)$ in the c.m. frame. Each datum point subtends 10°, while each distribution subtends about 2 MeV of photon energy. These distributions include the unresolved contribution from the inelastic reaction $^2\mathrm{H}(\gamma,\pi^0)np$. The curves represent the theoretical estimates for the inelastic cross section as described in Appendix B. An uncertainty of roughly $\pm 25\%$ is assigned to these estimates. Indicated photon energies are in the laboratory frame.

where $F(Q)$ is the deuteron structure form factor, $Q=|\vec{k}-\vec{q}|$ is the momentum transfer, $P_D=0.06$ is the D-state probability, and η is the frame-transformation factor defined by Eq. (A7).

As noted in Appendix A, the effective amplitude $\overline{E^{(+)}}$ is comprised of the ''bare'' nucleon amplitudes, the one- and two-nucleon rescattering contributions, and the P-wave-induced shift due to Fermi motion [Eq. (A15)]. In principle, $\overline{E^{(+)}}$ is a complex quantity even at low energy, but as argued in Appendix C, the imaginary part is negligible in the threshold region and therefore in the analysis all amplitudes in Eq. (15) will be treated as essentially real quantities.

Although the model cross section was evaluated in the PWIA, it is well known that final-state elastic pion-nucleus rescattering [i.e., distorted-wave impulse approximation (DWIA) corrections] can considerably enhance the PWIA cross sections, up to 28%, for example, in the $^{12}\mathrm{C}(\gamma,\pi^0)$ reaction [16]. Similar rescattering corrections have been evaluated for the $^2\mathrm{H}(\gamma,\pi^0)$ reaction by Kamalov *et al.* [10] and were found to be very small, apparently because of the small isoscalar πN scattering amplitude. Therefore, we will ignore the DWIA corrections and reserve comment for later.

Since it is obvious from Eq. (15) that the angular distributions do not permit a unique separation of the amplitudes $P_2^{(+)}$ and $P_3^{(+)}$, we have elected to combine them into a new amplitude H_0 defined by Eq. (A26). This is analogous (but not identical) to the amplitude F_0 invented for the analysis of the $^1\mathrm{H}(\gamma,\pi^0)$ measurements [3], defined by Eq. (A28). As noted in Appendix A, the particular form of H_0 yields a simple expression for the total cross section where all the P-wave contributions are lumped into a single term [just as F_0 serves in the total $^1\mathrm{H}(\gamma,\pi^0)$ cross section].

The differential cross section, Eq. (15), can be expressed in the form

$$\frac{k}{q}\frac{d\sigma}{d\Omega}=F^2(Q)(A+Bx+Cx^2), \tag{16}$$

where $x=\cos\theta$ and the coefficients are given by

$$A=\frac{4}{3}D^2[2(\eta\overline{E})^2-P_1^2]+8H_0^2,$$

$$B=\frac{16}{3}D^2\eta\overline{E}P_1,$$

$$C=4D^2P_1^2-8H_0^2, \tag{17}$$

and $D=1-\frac{3}{2}P_D$. The $(+)$ superscript has been suppressed for clarity, isovector-even amplitudes being understood. The analysis is now reduced to determining the three real quantities $\overline{E}^{(+)}$, $P_1^{(+)}$, and H_0 as a function of energy.

It is generally accepted that $P_{1,2,3}^{(+)}$ (and hence H_0) are smooth functions of energy. In particular, if $P_1^{(+)}$ and H_0 are *monotonic* functions of energy, this provides a powerful constraint on the general analysis of the angular distributions by enforcing continuity on two of the unknowns appearing in Eq. (17), which in turn reflects on the extraction of the principle amplitude $\overline{E}^{(+)}$. Enforcing continuity is most helpful very close to threshold where the P-wave contributions are otherwise subject to rather large experimental uncertainties. Such continuity was a constraint, for example, in the analyses of the ^{1}H(γ,π^0) experiments [3,4].

We will assume that the energy development of $P_1^{(+)}$ and H_0 in the threshold region can effectively be described by

$$P_1^{(+)}=p_1^{(+)}\cdot kq \tag{18}$$

and

$$H_0=h_0\cdot kq, \tag{19}$$

where k and q are the photon and pion momenta *in the πA frame* (expressed in units of the pion mass) and the ''reduced'' amplitudes $p_1^{(+)}$ and h_0 are presumed to be constants. The above follow directly (Appendix A) from the familiar ansatz wherein the free-nucleon amplitudes are proportional to *kq in the πN frame*. In Ref. [3] we demonstrated conclusively that the proton amplitude F_0 is very well described by the kq conjecture. In fact, we also demonstrated on theoretical grounds that F_0/kq *should* be nearly constant, varying by about 2% within 25 MeV of the ^{1}H(γ,π^0) threshold.

B. Energy-independent analysis

We begin by examining the energy dependence of the two P-wave amplitudes $P_1^{(+)}$ and H_0. We will demonstrate here that Eqs. (18) and (19) provide adequate descriptions of these amplitudes within 20 MeV of threshold and later will impose them as continuity constraints in an energy-dependent analysis of the angular distributions.

We proceed by fitting Eqs. (16) and (17) to the differential ^{2}H(γ,π^0)^{2}H cross sections, independently at each energy. These elastic cross sections are defined by the difference between the experimental cross sections of Fig. 3 and the indicated (theoretical) inelastic contributions. The resulting reduced amplitudes, expressed as $P_1^{(+)}/kq$ and H_0/kq, are plotted as a function of photon energy in Figs. 4 and 5,

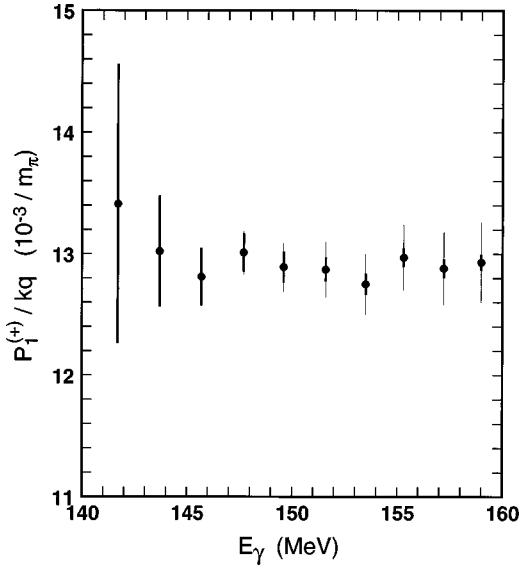

FIG. 4. Reduced amplitude $P_1^{(+)}/kq$ as a function of photon energy as deduced from the energy-independent analysis of the angular distributions. The heavy error bars are purely statistical in nature. The light bars reflect the $\pm 25\%$ uncertainty ascribed to the theoretical inelastic cross sections shown in Fig. 3.

respectively. The heavy error bars are purely statistical in nature, while the light bars define the systematic limits associated with the $\pm 25\%$ confidence level in the theoretical inelastic cross section. The statistical fluctuations increase significantly near threshold with diminishing P-wave strength. On the other hand, the systematic uncertainty increases with energy, reflecting the rapid growth of the inelastic cross section.

The results displayed in Figs. 4 and 5 support the energy dependence proposed by Eqs. (18) and (19). Whether or not these are the precise descriptions of $P_1^{(+)}$ and H_0 at low energy, they certainly represent very convenient approxima-

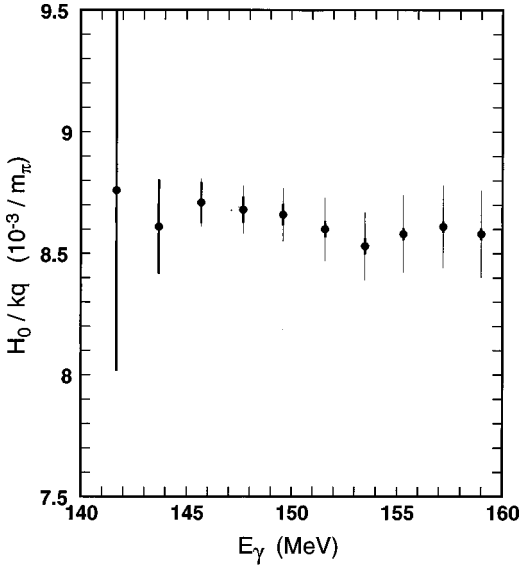

FIG. 5. Reduced amplitude H_0/kq as a function of photon energy as deduced from the energy-independent analysis of the angular distributions. The error bars are as described in Fig. 4.

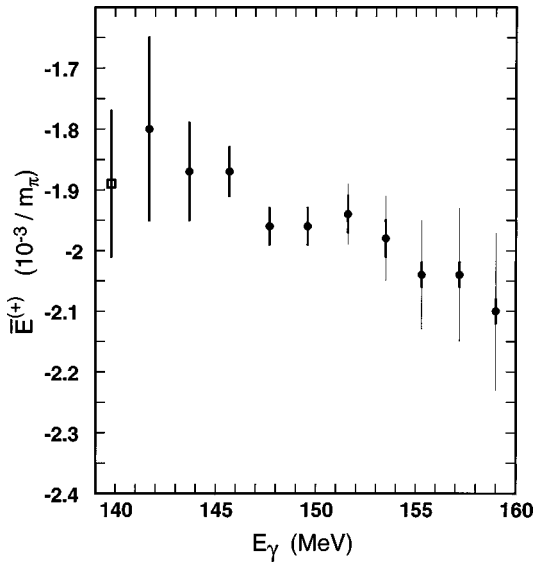

FIG. 6. Effective S-wave amplitude $\overline{E}^{(+)}$ as deduced from the energy-independent analysis of the angular distributions. The error bars are as described in Fig. 4. The square point is the threshold amplitude, Eq. (13), obtained from the total cross section.

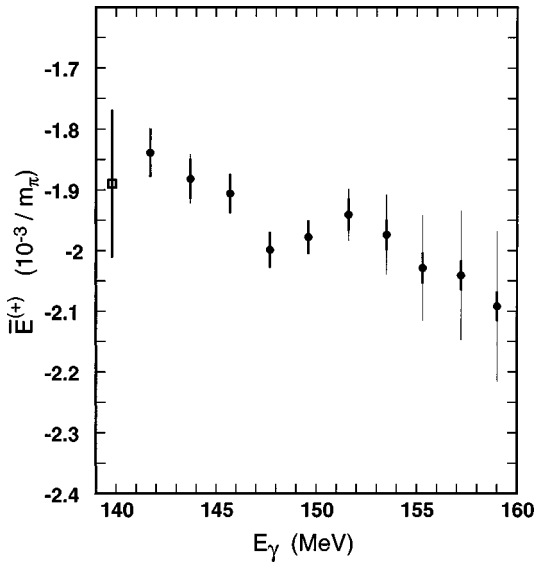

FIG. 7. Effective S-wave amplitude $\overline{E}^{(+)}$ as deduced from the energy-dependent analysis of the angular distributions. These quantities are treated as free parameters at each energy, but energy continuity of the P-wave amplitudes is now enforced through Eqs. (18) and (19). The error bars are as described in Fig. 4. The square point is the threshold amplitude, Eq. (13), obtained from the total cross section. The results portrayed here are indistinguishable from the amplitudes evaluated at $\theta=90°$ when the angular dependence from rescattering is incorporated in the analysis.

tions. Other representations are of course possible. For example, since the photon energy k is uniquely related to the pion momentum q, one could envisage a power-series representation in q^n, of necessarily odd order. From Figs. 4 and 5 it becomes clear that terms of order q^3 must be included in such an expansion.

Finally, in Fig. 6 we show the effective amplitude $\overline{E}^{(+)}$ as a function of energy. Also shown is the threshold amplitude, Eq. (13), deduced from the total cross section. Within statistics the two analyses are consistent.

C. Energy-dependent analysis

Energy continuity in the P-wave amplitudes will now be enforced using Eqs. (18) and (19). All elastic differential cross sections are fit simultaneously with Eqs. (16) and (17), where the amplitudes $\overline{E}^{(+)}$ are still free at each energy, but the reduced amplitudes $p_1^{(+)}$ and h_0 are treated as global constants. The quality of the fits is good—we obtain a reduced chi square of 1.2 for 180 data points and 12 free parameters, ignoring the systematic uncertainty in the inelastic contribution.

The reduced P-wave amplitudes from the energy-dependent analysis are

$$p_1^{(+)}=(12.88\pm0.28)\times10^{-3}/m_{\pi+} \tag{20}$$

and

$$h_0=(8.59\pm0.15)\times10^{-3}/m_{\pi+}\,, \tag{21}$$

where the indicated errors are dominated by the systematic uncertainty in the inelastic cross section. The above are in good agreement with the energy-independent amplitudes displayed in Figs. 4 and 5.

The effective S-wave amplitudes are shown in Fig. 7, where as before the heavy error bars are purely statistical and the light bars define the systematic limits. The present results are consistent with the amplitudes of Fig. 6, but display the expected statistical improvement at low energy from the P-wave continuity constraints.

From Fig. 7 one discerns a mild increase in $\overline{E}^{(+)}$ with energy, but more significantly there is no evidence for a unitarity cusp. The cusp should be most evident at $E_\gamma=146-147$ MeV from considerations of the corresponding free-nucleon S-wave amplitudes. For comparison, the $E_{0+}(\pi^0 p)$ amplitude from measurements of the $p(\gamma,\pi^0)$ reaction [2,3] varies by $\Delta E_{0+}\approx0.8\times10^{-3}/m_\pi$ between cusp extremes. This far surpasses the slight variation seen in Fig. 7, which is not considered statistically significant.

It is instructive to extrapolate the $\overline{E}^{(+)}$ amplitudes of Fig. 7 to threshold as a quantitative comparison of the current angular analysis with the total cross section analysis of Sec. III. For extrapolating functions we have employed both linear and quadratic polynomials in $E-E_{\rm th}$ where $E_{\rm th}$ is the threshold energy. Both functions yield virtually identical results, and we obtain

$$\overline{E}_{\rm th}^{(+)}=(-1.85\pm0.03)\times10^{-3}/m_{\pi+} \tag{22}$$

or, using Eq. (5),

$$E_d=(-1.42\pm0.02)\times10^{-3}/m_{\pi+}\,. \tag{23}$$

The systematic uncertainties in $\overline{E}^{(+)}$ have been ignored here. These results are in excellent agreement with our previous findings, Eqs. (12) and (13), perhaps indicating that the systematic uncertainties associated with the inelastic cross section are too conservative.

D. Angular dependence of $\overline{E}^{(+)}$

Until now we have treated the effective amplitude $\overline{E}^{(+)}$ solely as a function of energy. However, as noted in Sec. I, the two-nucleon rescattering term ΔE induces an angular dependence roughly in proportion to $1/F(Q)$, thus enhancing the back-angle amplitude relative to the forward amplitude. Here we will briefly consider how this angular dependence relates to our previous conclusions.

As outlined in Appendix A, the effective amplitude may be expressed as

$$\overline{E}^{(+)}=E_{0+}^{(+)}+\Delta E_p+\Delta E, \tag{24}$$

where the individual terms are given, respectively, by Eqs. (1), (A15), and (C5). The expression for ΔE [Eq. (C5)] depends on the ratio of expectation values, both of which are functions of angle. The denominator is identified as the deuteron form factor $F(Q)$ and is given by experiment [Eq. (A23)]. The numerator has been estimated using a Hulthén-type wave function. Empirically it is found that the numerator varies approximately as $F(Q)^{-\varepsilon}$ where $\varepsilon\approx 0.4$ and $F(Q)$ is the Hulthén form factor. We will assume that this functional dependence holds in general for more realistic wave functions, although in the final analysis the precise value of ε is not crucial.

The ansatz for $\overline{E}^{(+)}$ now assumes the form

$$\overline{E}^{(+)}=e_1+\frac{e_2}{F(Q)^{1+\varepsilon}}, \tag{25}$$

where $e_1=E_{0+}^{(+)}+\Delta E_p$ and e_2 is a free parameter defining the magnitude of ΔE.

The amplitude $E_{0+}^{(+)}$ is given by the ChPT nucleon amplitudes of Eq. (3). As noted previously, there is disagreement over the magnitude of the P-wave-induced shift ΔE_p. Beane *et al.* [7] conclude that ΔE_p is negligible, while our estimate $\Delta E_p\approx -0.3$ (Appendix A) is nearly sufficient to cancel the contribution from $E_{0+}^{(+)}$ in e_1. Both possibilities will therefore be considered.

A repeat of the energy-dependent analysis of the differential cross sections, but now incorporating the angular dependence implicit in Eq. (25), yields essentially the same chi square as before. The reduced P-wave amplitudes corresponding to the two possibilities for ΔE_p now become (in the usual units)

$$p_1^{(+)}=11.28\pm 0.28 \quad (\Delta E_p=0),$$

$$p_1^{(+)}=11.47\pm 0.28 \quad (\Delta E_p=-0.3) \tag{26}$$

and

$$h_0=8.28\pm 0.15 \quad (\Delta E_p=0),$$

$$h_0=8.31\pm 0.15 \quad (\Delta E_p=-0.3). \tag{27}$$

Compared with our initial results, Eqs. (20) and (21), the only notable change is a decrease in $p_1^{(+)}$. As discussed later, theoretical predictions for $p_1^{(+)}$ for the free nucleon fall well below our initial finding. However, the above values of $p_1^{(+)}$ reduce the discrepancy with theory somewhat, perhaps indirectly affirming the angular dependence of $\overline{E}^{(+)}$.

Since the present amplitudes $\overline{E}^{(+)}$ are a function of angle, direct comparison with the previous amplitudes is problematical. Assuming the amplitudes evaluated at $\theta=90°$ are representative, we find negligible differences from the results displayed in Fig. 7. This is not unexpected since, as seen from Eq. (15), the $P_1^{(+)}$ term vanishes at $\theta=90°$ and hence no trade-off between $\overline{E}^{(+)}$ and $P_1^{(+)}$ can occur here. The stability of $\overline{E}^{(+)}$ at $\theta=90°$ to the variations in ΔE_p simply reflects an exchange of strength between the e_1 and e_2 coefficients in Eq. (25) in a manner which conserves the amplitude.

In summary, the angular dependence of $\overline{E}^{(+)}$ introduced by the two-nucleon rescattering correction ΔE reduces our estimate of the P-wave amplitude $p_1^{(+)}$, but otherwise our previous conclusions remain essentially unchanged.

V. DISCUSSION

The backward enhancement of the pion angular distributions is proof that the electric dipole amplitude is negative in sign in the threshold region, in agreement with the sign predicted by the ChPT calculation of Ref. [7]. Furthermore, the experimental value for the threshold amplitude E_d is only about 20% below the ChPT estimate, testifying to the dominant role played by rescattering, as indeed had long been predicted [5].

Above threshold, the effective S-wave amplitude $\overline{E}^{(+)}$ shows no indication of the unitarity cusp that is so prominent in the proton amplitude [2–4] and, presumably, also in the neutron amplitude. Elementary considerations dictate that the nucleon cusp modulations combine constructively in the deuteron. The absence of any structure in $\overline{E}^{(+)}$ is therefore an indication that those particular manifestations of isospin breakdown which are responsible for the nucleon cusps are somehow subdued in the deuteron.

One might argue that the deuteron cusp has been washed out by the Fermi motion of the nucleons. While it is plausible that Fermi motion has a diluting influence, it would be surprising if it were sufficient to remove virtually *all* evidence of the deep nucleon cusps.

A more plausible argument for the absence of the deuteron cusp builds on an analogy with the free nucleon and hinges on unitarity. As noted in Appendix C, the nucleon S-wave amplitudes E_{0+} acquire imaginary components from the loop diagrams as described by Eq. (C3), where $\overline{q}$ in these expressions is the on-shell momentum of the virtual charged pion. Isospin breakdown splits the pion masses, and below the charged-pion threshold one replaces $\overline{q}\rightarrow i|\overline{q}|$ as dictated by analyticity. It follows that below the $\pi^{\pm}$ threshold the terms described by Eq. (C3) contribute only to the *real* amplitudes, in effect generating the unitarity cusps in $\mathrm{Re}\,E_{0+}$. Of course, this is an oversimplification since we are ignoring the underlying off-shell dynamics, but it serves to illustrate the connection between $\mathrm{Im}\,E_{0+}$ and $\mathrm{Re}\,E_{0+}$ on either side of the $\pi^{\pm}$ thresholds. Now let us apply these concepts to the deuteron. If the deuteron were a truly structureless isoscalar particle, then the imaginary amplitude would necessarily vanish (neglecting π^0 loops) and, hence, the cusp as well.

The deuteron, of course, is not structureless, but as argued in Appendix C, the imaginary amplitude is still expected to be quite small. Pressing the free-nucleon analogy, the cusp would therefore also be small. This hypothesis is made more quantitative by reference to Appendix C, where we demonstrate a cancellation between the one- and two-nucleon rescattering terms at order $\overline{q}$, which remains in effect in the region below the charged-pion threshold as well. The cancellation of terms of order $\overline{q}$ in the deuteron but not the nucleon is significant because, as one recalls, it is the rapid energy dependence of $|\overline{q}|$ between the π^0 and π^+ thresholds that generates the free-proton cusp, at least in the simple K-matrix picture. In this picture, then, the same mechanism that suppresses the imaginary part of $\overline{E}^{(+)}$ in the deuteron above the $\pi^\pm$ threshold also suppresses the cusp in Re $\overline{E}^{(+)}$ below threshold.

Let us now turn to the P-wave amplitudes $P_1^{(+)}$ and H_0. The latter is comprised of $P_{1,2,3}^{(+)}$ and the deuteron D-state probability [Eq. (A26)], and was introduced to express the differential cross section more conveniently in terms of three separable amplitudes.

From the energy-independent analysis of the differential cross sections, we have demonstrated that $P_1^{(+)}$ and H_0 are very well parametrized by the expressions (18) and (19) in the threshold region. This finding lends support to the key conjectures underlying the model cross section of Appendix A, since those conjectures ultimately lead to an identical parametrization of these amplitudes [see Eqs. (A8)–(A13)]. Our comparison with theory will therefore be made through the reduced amplitudes $p_1^{(+)}$ and h_0.

The reduced P-wave amplitudes for free nucleons have been calculated *at threshold* in ChPT [11,17], and where comparison with experiment has been feasible, agreement is generally observed within a few percent or so [2,3,14]. In other words, the predictive power of ChPT in this sector appears to be rather good and defines the basis for the following discussion.

The ChPT estimates for the reduced nucleon amplitudes of interest are (in units of $10^{-3}/m_\pi$)

$$p_1^{(+)}=8.9,$$

$$h_0=7.5, \tag{28}$$

where h_0 was evaluated for a 6% D-state probability. These amplitudes are considerably lower than the initial experimental findings represented by Eqs. (20) and (21). The comparison improves, especially for $p_1^{(+)}$, when the angular dependence of $\overline{E}^{(+)}$ is taken into account as reflected in the revised amplitudes of Eqs. (26) and (27). Nevertheless, a substantial discrepancy with theory is still evident, and we comment on the possible origin.

First, let us note the ChPT predictions for each of the isovector-even amplitudes [11,17]:

$$p_1^{(+)}=8.9, \quad p_2^{(+)}=-9.7, \quad p_3^{(+)}=11.4. \tag{29}$$

The amplitude $p_3^{(+)}$ was not explicitly calculated in ChPT—rather it was assembled as described in Ref. [14] from the proton amplitude together with known relations between the so-called low-energy constants. The experimental estimate for $p_3^{(+)}$ as deduced from the $^{12}\mathrm{C}(\gamma,\pi^0)$ reaction [14] is in excellent agreement with Eq. (29), and so we have no *a priori* reason to suspect $p_3^{(+)}$. Attention thus shifts to the other two amplitudes.

Unlike $P_3^{(+)}$, both $P_1^{(+)}$ and $P_2^{(+)}$ are associated with the spin-dependent part of the elementary transition operator [Eqs. (A2) and (A3)]. Moreover, from the defining equations (2) we have the approximate relation $P_2^{(+)}\approx -P_1^{(+)}$ since the multipole $E_{1+}^{(+)}$ is small. Let us therefore propose that the ChPT amplitude $P_2^{(+)}$ suffers the same (relative) upward renormalization as we perceive in the experimental value of $P_1^{(+)}$ in comparing Eq. (26) with Eq. (28). A reevaluation of h_0, now using the experimental estimate for $p_1^{(+)}$, the renormalized ChPT value for $p_2^{(+)}$, and the unaltered ChPT value for $p_3^{(+)}$, yields the result

$$h_0=8.4, \tag{30}$$

which compares much more favorably with the experimental result, Eq. (27), than does the unmodified ChPT amplitude of Eq. (28). The argument is crude, but it does point to *both* $p_1^{(+)}$ and $p_2^{(+)}$ as the sources of the discrepancy with theory.

The apparent upward renormalization of $p_{1,2}^{(+)}$ relative to the free-nucleon amplitudes, as inferred from the deuteron photopion reaction, is suggestive of some sort of two-body contribution which goes beyond the usual impulse approximation. Two-body contributions to the $d(\gamma,\pi^0)d$ reaction have been explored by Wilhelm and Arenhövel [18], and although they focus on higher energies than here, some aspects may pertain to the threshold region. Of note is the process wherein the photon couples to one nucleon while the pion is emitted by the other. As discussed in [18], this is a nonresonant mechanism, which means it would influence $P_1^{(+)}$ and $P_2^{(+)}$ but not $P_3^{(+)}$ since the latter amplitude is almost exclusively driven by the $\Delta(1232)$. While consistent with our above hypothesis, there is a serious drawback. According to [18], the ''crossed'' diagram nearly cancels the forward diagram, suggesting a small residual two-body amplitude. We are unaware of any such estimates at low energy that also reflect the off-shell nature of the bound nucleons.

Finally, two recent theoretical developments deserve mention. The first [19] is an investigation of the threshold photoproduction of pions from the nucleon using fixed-t dispersion relations. Threshold amplitudes were predicted by fitting to experiment in the energy range 160–420 MeV. From those results we deduce $p_1^{(+)}=9.2$, which agrees nicely with the ChPT prediction, Eq. (28), and reaffirms the discrepancy with the present finding. No description of p_3 is given, and so we can not comment on h_0.

In the other development [20], unitarity arguments are used to calculate the imaginary contribution to E_d from the virtual process $\gamma d\rightarrow np\rightarrow\pi^0 d$. Although the resulting change in the cross section is small, the author notes that the real amplitude should also be affected by the process. No one has yet calculated the effect on E_d, but if large, it could have an impact upon the ChPT prediction. This is relevant since as we have seen, our relative agreement with the ChPT amplitude favored the ChPT estimate for the neutron amplitude

$E_{0+}(\pi^0 n)$ over the classical LET prediction. A better understanding of the role of the np channel is clearly called for.

As emphasized in [20], the threshold amplitude is actually comprised of two distinct components—the familiar electric dipole ($E1$) amplitude plus a magnetic quadrupole ($M2$) amplitude as permitted by the $1^+ \rightarrow 1^-$ nature of the hadronic transition. Since the two amplitudes combine incoherently in the total cross section, our result for E_d [Eq. (12)] must be interpreted as an upper limit on the $E1$ contribution.

We conclude with a comment about the model cross section which was employed in the analysis of the differential cross sections. As stated in Sec. IV, the DWIA corrections from elastic pion-nucleus rescattering were ignored. Such effects tend to increase the cross section due to the attractive nature of the pion-nucleus interaction, and so their inclusion tends to reduce the amplitudes as deduced from experiment. A feeling for the sensitivity is given by an example. Let us assume the DWIA correction increases linearly with energy, reaching a maximum of 10% at our highest energy. Under reanalysis, the amplitudes $\overline{E}^{(+)}$, $p_1^{(+)}$, and h_0 shifted at most by 4%, while the chi square worsened. Interestingly, the optimal chi square occurs when there is no slope to the hypothetical DWIA correction.

VI. CONCLUSION

We present new measurements of both the total and differential cross sections for the reaction $^2H(\gamma,\pi^0)$ within 20 MeV of threshold. The total cross section is in general agreement with the only previous measurement [1], but is of greatly improved statistical quality. No previous angular distributions have been reported in the threshold region.

One focus of the present investigation is the effective S-wave photoproduction amplitude $\overline{E}^{(+)}$ for the elastic reaction $^2H(\gamma,\pi^0)^2H$ both at threshold and above threshold. The necessary formulation for comparison with the experimental cross sections and a theoretical estimate for the unresolved inelastic contribution $^2H(\gamma,\pi^0)np$ are developed in the Appendixes. Included there is an estimate of the imaginary part of $\overline{E}^{(+)}$, shown to be relatively small and therefore neglected in the analysis. It must be noted, however, that if the estimates for Im $\overline{E}^{(+)}$ are in serious error, then certain of our conclusions could be compromised, in particular the deduced energy dependence of the P-wave amplitudes as portrayed by Figs. 4 and 5.

The threshold amplitude E_d has been deduced from separate analyses of the total and differential cross sections, with mutually consistent results. The experimental value falls about 20% below the electric dipole amplitude predicted by chiral perturbation theory [7], but agrees in sign (negative). The discrepancy may originate in part in the theoretical treatment of the two-nucleon charge-exchange rescattering correction. Until this is under better control, the best we can say concerning the neutron amplitude $E_{0+}(\pi^0 n)$ is that the present results favor the ChPT prediction over the classical LET prediction. Besides the rescattering contribution, other factors still require careful theoretical consideration, for example, the precise role of Fermi motion, the contribution from the two-step process $\gamma d \rightarrow pn \rightarrow \pi^0 d$, and the magnetic quadrupole contribution to the threshold amplitude.

Analysis of the differential cross sections proceeded in three stages. The familiar ansatz wherein the energy development of P-wave multipoles is proportional to kq was confirmed for the two particular amplitudes of concern here, and this was subsequently utilized as a continuity constraint in the energy-dependent fits. For the final analysis, the effective amplitude $\overline{E}^{(+)}$ was permitted to vary with angle in accordance with the two-nucleon rescattering correction ΔE.

Significantly, all three analyses returned nearly the same central values for the $\overline{E}^{(+)}$ (the errors, however, change as expected). The results show a mild monotonic increase with energy, but display no evidence of a unitarity cusp. The absence of a cusp was resolved by a simple argument based in part on the K-matrix formalism, but this needs a more rigorous theoretical treatment.

The initial estimate for the reduced P-wave amplitude $p_1^{(+)}$ as deduced from the angular distributions is much larger than the corresponding free-nucleon amplitude predicted by ChPT. The gap is reduced somewhat when the angular dependence of $\overline{E}^{(+)}$ is incorporated in the analysis and is further reduced if the DWIA corrections to our PWIA model cross section are not negligible, as we have assumed. However, even under the most optimistic scenario there remains a discrepancy of roughly 20%. A smaller but still significant discrepancy remains in the amplitude h_0.

We have suggested that the problem lies with the two amplitudes $p_1^{(+)}$ and $p_2^{(+)}$, but not with $p_3^{(+)}$. One mechanism seemingly capable of renormalizing the former amplitudes but not the latter is the two-body process where the photon reacts with one nucleon while the pion is emitted by the other. This explanation, however, appears compromised, due to a strong cancellation with the ''crossed'' diagram [18], and we have no estimate of the residual two-body amplitude in the threshold region. We hope that the present measurements will encourage further theoretical developments in the threshold region.

Tabulated values of the total and differential cross sections (including or excluding the inelastic component) are available on the SAL webpage at http://sal.usask.ca.

ACKNOWLEDGMENTS

We wish to thank the SAL staff whose hard work in providing the high quality cw beam from the pulse-stretcher ring made this experiment possible. Special thanks go to Dr. E. Hallin and Dr. G. Retzlaff who provided help and advice with many of the experimental details. Stimulating discussions with Dr. E. L. Tomusiak and Dr. M. Benmerrouche about the theory for this reaction are also gratefully acknowledged. This work was performed in part with a grant supplied by the Natural Sciences and Engineering Research Council (NSERC).

APPENDIX A: ELASTIC CROSS SECTION

We describe here the construction of the model cross section for $^2H(\gamma,\pi^0)^2H$ at low energies. The model is founded on the usual impulse approximation in which free-nucleon amplitudes describe photoproduction from each bound nucleon. The model then evolves to incorporate the deuteron structure, the transformation from the πN to πA frames, and

Fermi motion, all in various degrees of approximation. A quantitative treatment of those issues lies beyond the scope of the present paper. Rather, we seek a qualitative description that is sufficient for our purpose, in particular one that clearly reflects the underlying nucleon amplitudes.

The differential cross section is given by the general expression

$$\frac{k}{q}\frac{d\sigma}{d\Omega}=\frac{1}{2(2J_i+1)}\sum_{\lambda MM'}\left|\langle d|\sum_i M_{\gamma\pi}(i)|d\rangle\right|^2, \quad \text{(A1)}$$

where λ, M, and M' are the photon and deuteron spin projections, $J_i=1$ is the deuteron spin, and $M_{\gamma\pi}(i)$ is the nucleon photoproduction operator. The latter may be written

$$M_{\gamma\pi}(i)=i\vec{\sigma}\cdot\vec{K}+L, \quad \text{(A2)}$$

where

$$\vec{K}=\hat{\varepsilon}_\lambda(E_{0+}+\hat{k}\cdot\hat{q}P_1)+\hat{k}(\hat{\varepsilon}_\lambda\cdot\hat{q})P_2,$$

$$L=(\hat{q}\times\hat{k})\cdot\hat{\varepsilon}_\lambda P_3. \quad \text{(A3)}$$

The P-wave amplitudes $P_{1,2,3}$ are the proton and neutron equivalents of Eq. (2), and at this stage all quantities in Eq. (A3) are defined in the pion-nucleon (πN) frame. Ignoring the nuclear structure of the deuteron for the moment, Eqs. (A1)–(A3) yield the prototype cross section

$$\frac{k}{q}\frac{d\sigma}{d\Omega}=\frac{8}{3}(E_{0+}^{(+)}+P_1^{(+)}\cos\theta^*)^2+\frac{4}{3}(P_2^{(+)}\sin\theta^*)^2$$

$$+2(P_3^{(+)}\sin\theta^*)^2, \quad \text{(A4)}$$

where $A^{(+)}$ in general denotes the isovector-even amplitudes [recall Eq. (1)] and θ^* is the pion angle in the πN frame.

Next, we transform from the πN frame to the πA (pion-nuclear) frame, but this cannot be decoupled from consideration of the Fermi motion. For the latter we resort to the so-called *factorization approximation*, which simply assumes

$$\vec{P}_f=-\vec{P}_i, \quad \text{(A5)}$$

these being the final and initial momenta of the active nucleon in the frame of the nucleus. Invoking the impulse approximation together with Eq. (A5), one finds [16,21]

$$\vec{P}_i=-\frac{1}{2}\left(1-\frac{1}{A}\right)\vec{Q}, \quad \text{(A6)}$$

where $\vec{Q}=\vec{k}-\vec{q}$ is the momentum transfer in the πA frame and $A=2$ for the deuteron. The approximation encompassed by Eqs. (A5) and (A6) has been tested against explicit treatments of Fermi motion to quite satisfactory effect as demonstrated, for example, in Refs. [10, 21].

Under the transformation to the πA frame, all amplitudes in Eq. (A3) acquire a factor η, which in the threshold region is given by

$$\eta\approx\frac{1+m_\pi/m}{1+m_\pi/m_d}=1.07, \quad \text{(A7)}$$

where m_π, m, and m_d are the pion, nucleon, and deuteron masses. This factor originates from the convention of absorbing the phase-space factor m/W into the definition of the free amplitudes, where W is the πN invariant mass.

Transformation of Eq. (A3) to the πA frame is quite straightforward if we assume that the P-wave amplitudes follow the familiar low-energy conjecture

$$P_j=p_j\cdot k^*q^* \quad (j=1-3), \quad \text{(A8)}$$

where the ''reduced'' amplitudes p_j (different for the proton and neutron) are presumed to be constants and the momenta k^* and q^* are defined in the πN frame. The momentum dependence of Eq. (A3) is then confined to terms proportional to $\vec{q}^*\times\vec{k}^*$ and $\vec{q}^*\cdot\vec{k}^*$. The Lorentz transformations of $\vec{q}^*$ and $\vec{k}^*$ to the πA frame have been described elsewhere [16]. Those transformations together with the factorization approximation then yield

$$\vec{q}^*\times\vec{k}^*\approx\frac{1}{\eta}\vec{q}\times\vec{k}, \quad \text{(A9)}$$

$$\vec{q}^*\cdot\vec{k}^*\approx\frac{1}{\eta^2}(\vec{q}\cdot\vec{k}-\varepsilon Q^2), \quad \text{(A10)}$$

where, to order m_π^2,

$$\varepsilon=\frac{m_\pi}{4m}\left(1-\frac{m_\pi}{4m}\right). \quad \text{(A11)}$$

The photon and pion momenta, $\vec{k}$ and $\vec{q}$, respectively, are defined in the πA frame and the nuclear momentum transfer is defined by $\vec{Q}=\vec{k}-\vec{q}$. The term proportional to ε originates from our treatment of Fermi motion. To order m_π it is identical to the corresponding term arising from the so-called ''angle transformation'' in pion-nucleus scattering [8].

The prototype cross section, Eq. (A4), now becomes

$$\frac{k}{q}\frac{d\sigma}{d\Omega}=\frac{8}{3}\left[\eta E_{0+}^{(+)}+\frac{1}{\eta}P_1^{(+)}\left(\cos\theta-\varepsilon\frac{Q^2}{kq}\right)\right]^2$$

$$+\frac{4}{3}(P_2^{(+)}\sin\theta)^2+2(P_3^{(+)}\sin\theta)^2, \quad \text{(A12)}$$

where θ is the pion angle in the πA frame and the P-wave amplitudes are

$$P_j^{(+)}=p_j^{(+)}\cdot kq. \quad \text{(A13)}$$

The reduced isovector-even amplitudes $p_j^{(+)}$ are directly related to the corresponding free nucleon p_j of Eq. (A8).

Note that even at threshold the Fermi term proportional to ε remains finite. Above threshold, it may be expanded into angular-dependent and isotropic terms. Let us adopt the convention that in the πA frame the effective P-wave amplitudes vanish at threshold. It is then necessary to absorb the isotropic parts of the Fermi term into a redefinition of the S-wave amplitude,

$$\overline{E}^{(+)}=E_{0+}^{(+)}+\Delta E_p, \quad \text{(A14)}$$

where

$$\Delta E_p = -\frac{\varepsilon}{\eta^2}(k^2+q^2)\frac{P_1^{(+)}}{kq} \tag{A15}$$

and $P_1^{(+)}$ is defined by Eq. (A13). In effect, the P waves ''induce'' a shift ΔE_p in the S-wave amplitude due to the Fermi motion, where $\Delta E_p \approx -0.3\times 10^{-3}/m_{\pi^+}$ at threshold. We note in passing that a term very similar to Eq. (A15) follows from the work of Koch and Woloshyn [5] when one imposes the factorization approximation, Eqs. (A5) and (A6), upon their direct term.

The effective S-wave amplitude $\overline{E}^{(+)}$ is still incomplete since rescattering has so far been ignored. We assume the two-nucleon rescattering contribution ΔE described in Sec. I modifies the effective amplitude in simple additive fashion,

$$\overline{E}^{(+)} = E_{0+}^{(+)} + \Delta E_p + \Delta E. \tag{A16}$$

Finally, one-nucleon rescattering is automatically included in $E_{0+}^{(+)}$ if, for example, we adopt the ChPT amplitudes of Eq. (3).

In terms of the effective S-wave amplitude represented by Eq. (A16), the prototype cross section to good approximation becomes

$$\frac{k}{q}\frac{d\sigma}{d\Omega} = \frac{8}{3}(\eta\overline{E}^{(+)} + P_1^{(+)}\cos\theta)^2 + \frac{4}{3}(P_2^{(+)}\sin\theta)^2 + 2(P_3^{(+)}\sin\theta)^2. \tag{A17}$$

The deuteron nuclear structure enters the cross section through four structure form factors [22]. Two form factors are of the monopole type and correspond to $S\rightarrow S$ and $D\rightarrow D$ transitions between the deuteron S and D states. The other form factors are of the quadrupole type and include $S\leftrightarrow D$ transitions. The quadrupole terms are negligible near threshold and will not be considered further. The monopole form factors are defined by

$$F_1(Q) = \int dr\, j_0\left(\frac{1}{2}Qr\right)[u^2+w^2],$$

$$F_2(Q) = \int dr\, j_0\left(\frac{1}{2}Qr\right)\left[u^2 - \frac{1}{2}w^2\right], \tag{A18}$$

where u and w are the usual radial wave functions. The form factor F_1 is associated with the L term of Eq. (A3) while F_2 is associated with the $\vec{K}$ term. Thus F_1 will only modulate the $P_3^{(+)}$ term in the prototype cross section, Eq. (A17), while F_2 modulates all other terms. If one neglects the D state, then clearly $F_2 = F_1$.

The D state is easily accommodated to good approximation in the threshold region. Denoting the D-state probability by P_D, we have the identity

$$F_2(Q) = \left(1-\frac{3}{2}P_D\right)F_1(Q) - \frac{3}{2}P_D(1-P_D)G(Q), \tag{A19}$$

where

$$G(Q) = \frac{1}{6}Q^2 r_S^2\left\{1-\left(\frac{r_D}{r_S}\right)^2\right\} + \cdots \tag{A20}$$

is a rapidly converging power series. Here r_S and r_D are, respectively, the rms radii of the S and D states u and w when the latter are individually normalized to unity. For example, for the Paris potential one finds $r_S = 2.01$ fm and $r_D = 1.25$ fm, with other potentials yielding similar values. The final term in Eq. (A19) amounts to a correction of about 2%, which we will ignore, this being a much better approximation than if we had set $P_D = 0$ everywhere. [The correction is actually smaller than 2% since the next term in Eq. (A20) is negative in sign.] Thus we may write

$$F_2(Q) \approx \left(1-\frac{3}{2}P_D\right)F_1(Q) \tag{A21}$$

and the differential cross section takes its final form

$$\frac{k}{q}\frac{d\sigma}{d\Omega} = F^2(Q)\left\{\left(1-\frac{3}{2}P_D\right)^2\left[\frac{8}{3}(\eta\overline{E}^{(+)} + P_1^{(+)}\cos\theta)^2 + \frac{4}{3}(P_2^{(+)}\sin\theta)^2\right] + 2(P_3^{(+)}\sin\theta)^2\right\}, \tag{A22}$$

where $F(Q) = F_1(Q)$. Note that the D-state contribution reduces the cross section near threshold by about 17% (for $P_D = 0.06$) and therefore cannot be neglected. In writing Eq. (A22) we are treating the effective amplitude $\overline{E}^{(+)}$ as a real quantity. In principle, of course, it is a complex quantity, but as demonstrated in Appendix C, the imaginary component is expected to be small in the threshold region.

The structure form factor $F(Q)$ may be deduced from the electron scattering results of Simon *et al.* [23] after the proton charge form factor is removed. For the momentum transfer region $Q^2 \leqslant 1.55$ fm^{-2}, we achieve an excellent description using the phenomenological function

$$F^2(Q) = e^{-Q^2r^2/3}(1+pQ^4), \tag{A23}$$

with $r = 1.90$ fm and $p = 0.317$ fm^4. The parameter r may be compared with the rms structure radius $\langle r_d^2\rangle^{1/2} = 1.96$ as deduced by Simon *et al.* [23]. At pion threshold we obtain $F(k) = 0.79$, in agreement with the value employed by Beane *et al.* [7].

The cross section given by Eq. (A22) can be expressed as

$$\frac{k}{q}\frac{d\sigma}{d\Omega} = F^2(Q)(A+Bx+Cx^2), \tag{A24}$$

where $x = \cos\theta$ and the coefficients A, B, and C are functions of the multipole amplitudes. The form factor $F(Q)$, however, is also a function of angle, and so extraction of the coefficients from the angular distributions is not as clear-cut as in the $p(\gamma,\pi^0)$ measurements [2].

The coefficients $A-C$ are defined by

$$A=\frac{8}{3}D^2(\eta\overline{E})^2+\frac{2}{3}(2D^2P_2^2+3P_3^2),$$

$$B=\frac{16}{3}D^2(\eta\overline{E}P_1),$$

$$C=\frac{2}{3}(4D^2P_1^2-2D^2P_2^2-3P_3^2), \tag{A25}$$

where $D=1-\frac{3}{2}P_D$ and the $(+)$ indicator has been removed for brevity, isovector-even amplitudes being understood everywhere. The P-wave amplitudes in the πA frame have been previously defined through Eq. (A13).

One sees from the above expressions that the D factor in effect renormalizes each of the multipole amplitudes (except P_3) by about 9%. Since it is also apparent that P_2 and P_3 cannot be isolated, we will combine them into a single quantity, thus forming a third independent amplitude. This composite amplitude is defined by

$$H_0^2=\frac{1}{6}\left\{D^2(P_1^2+P_2^2+P_3^2)+\left(\frac{3}{2}-D^2\right)P_3^2\right\}, \tag{A26}$$

and the coefficients of Eq. (A25) now assume the form given by Eq. (17). The differential cross section thus becomes a function of the (separable) amplitudes $\overline{E}^{(+)}$, $P_1^{(+)}$, and H_0.

The total cross section may be expressed in terms of these amplitudes in the approximate form

$$\frac{k}{q}\sigma\approx 4\pi\frac{8}{3}\langle F^2\rangle(D^2\eta^2|\overline{E}^{(+)}|^2+2H_0^2), \tag{A27}$$

where $\langle F^2\rangle$ denotes the angular mean value of $F^2(Q)$. The peculiar definition of H_0^2 was chosen, in part, in order to consolidate all the πN P-wave amplitudes into a single term in the total cross section. A similar construction was incorporated in our treatment of the $p(\gamma,\pi^0)$ cross section [3], where the amplitude corresponding to H_0^2 was defined by

$$F_0^2=\frac{1}{6}(P_1^2+P_2^2+P_3^2), \tag{A28}$$

proton amplitudes being understood for $P_{1,2,3}$. The total $p(\gamma,\pi^0)$ cross section is then given by

$$\frac{k}{q}\sigma=4\pi(|E_{0+}|^2+2F_0^2), \tag{A29}$$

similar in structure to the deuteron cross section, Eq. (A27).

Finally, in Ref. [3] we demonstrated that the behavior of F_0 within 25 MeV of threshold was well described by the expression

$$F_0=f_0\cdot kq, \tag{A30}$$

where the reduced amplitude f_0 is a constant. Since the quadratic sum of $P_{1,2,3}$ is also the predominant component of H_0^2, we assume a similar low-energy ansatz

$$H_0=h_0\cdot kq, \tag{A31}$$

where the reduced amplitude h_0 is presumed constant. Note, however, that unlike F_0, the quantity H_0 is a function of the isovector-even amplitudes $P_j^{(+)}$.

APPENDIX B: INELASTIC CROSS SECTION

In this appendix we calculate the cross section for the inelastic reaction $^2\mathrm{H}(\gamma,\pi^0)np$ where the final state nucleons are not observed. To the best of our knowledge, no previous calculation of this particular reaction in the threshold region exists in the literature. Our model is admittedly rather simplistic. For example, we will employ square-well wave functions and use the effective range approximation to describe the final-state n-p interaction. Final-state π^0N interactions are ignored since the respective scattering lengths are very small. The deuteron D state is ignored, and the relative n-p angular momenta are confined to S, P, and D waves.

The transition operator is again given by Eqs. (A2) and (A3), and in fact much of the formalism for the elastic reaction presented in Appendix A may be adopted to the present calculation, with the appropriate modifications for the final-state continuum.

For a given photon energy k, energy conservation in the photon-deuteron c.m. frame gives

$$k+\frac{k^2}{2m_d}=B+E_\pi+\frac{q^2}{8\mu}+\frac{p^2}{2\mu}, \tag{B1}$$

where $E_\pi=(m_\pi^2+q^2)^{1/2}$, $B=2.225$ MeV is the binding energy, μ is the N-N reduced mass, and p denotes the momentum of either nucleon in the final n-p center of mass frame. Since the nucleons are unobserved, we must integrate over their final degrees of freedom, and from energy conservation this implies integration over the pion momentum q. For given k, the maximum value of p (denoted $p_{\max}$) occurs when $q=0$ as seen from Eq. (B1). Using the elastic cross section, Eq. (A22), as a starting point, the unobserved n-p continuum is incorporated through the substitution

$$qF^2(Q)\rightarrow\frac{1}{(2\pi)^3}\int_0^{p_{\max}}q|F_T(Q)|^2p^2dp\;d\Omega_p, \tag{B2}$$

where $F_T(Q)$ is now a (complex) transition form factor. Of course, the multipole amplitudes in Eq. (A22) must eventually be incorporated into the integrand since they depend on q.

The total n-p spin can be $S=0$ (singlet) or $S=1$ (triplet), and each introduces a different spin factor into the cross section. For the singlet state, an extra factor of 1/2 must be included in Eq. (A22) and the term proportional to P_3 is absent.

The transition form factor is

$$F_T(Q)=\langle\Psi_f|e^{i\vec{\mathbf{Q}}\cdot\vec{\mathbf{r}}/2}|\Psi_d\rangle, \tag{B3}$$

where Ψ_d is the $^3S_1$ deuteron spatial wave function and Ψ_f is the n-p continuum wave function. For the moment we ignore all final-state interactions and write

$$\Psi_f=e^{i(\vec{\mathbf{p}}\cdot\vec{\mathbf{r}})}, \tag{B4}$$

where $\vec{p}$ is the momentum of either nucleon in the N-N c.m. frame and $\vec{r}$ is the relative nucleon separation.

Next, we consider the integration over Ω_p in Eq. (B2). This is elementary since the orientation of $\vec{q}$ is independent of the direction of $\vec{p}$, and consequently the sole Ω_p dependence resides in Ψ_f. We expand Ψ_f and the exponential term of Eq. (B3) in separate partial-wave series, and after some manipulation obtain

$$\int |F_T(Q)|^2 d\Omega_p = 4\pi \sum_l (2l+1)|f_l(Q)|^2, \quad \text{(B5)}$$

where

$$f_l(Q) = \int j_l(pr) j_l(Qr/2) \Psi_d d\vec{r} \quad \text{(B6)}$$

and l denotes the relative n-p orbital angular momentum. The above assumes a purely S-state deuteron with normalization

$$\int |\Psi_d|^2 d\vec{r} = 1.$$

Since we will wish to classify the final n-p continuum (and the cross section) according to isospin, it is necessary to consider the spin-isospin symmetry of the individual terms in the sum over l in Eq. (B5). A given isospin separates the terms into singlet and triplet spin states according to the value of l. As noted, these spin states differ by a factor of 1/2 in their respective cross sections. It is convenient to absorb this factor into the isospin decomposition of Eq. (B5), which we write as

$$\int |F_T(Q)|^2 d\Omega_p = 4\pi \left(f_0^2 + \frac{3}{2} f_1^2 + 5 f_2^2 + \cdots \right)_{T=0}$$
$$= 4\pi \left(\frac{1}{2} f_0^2 + 3 f_1^2 + \frac{5}{2} f_2^2 + \cdots \right)_{T=1}, \quad \text{(B7)}$$

where T denotes the total n-p isospin and the (real) partial-wave form factors are given by Eq. (B6) in the absence of final-state interactions.

Transitions to the $T=0$ and $T=1$ final states are driven by the isovector-even amplitudes $A^{(+)}$ and the isoscalar amplitudes $A^{(0)}$, respectively, these quantities differing only in the relative sign between the proton and neutron amplitudes [recall Eq. (1)]. The respective inelastic cross sections follow directly by substituting Eq. (B2) with Eq. (B7) into Eq. (A22), together with the appropriate S- and P-wave amplitudes $A^{(+,0)}$. The integral over p must, of course, encompass these amplitudes. The resulting expressions are rather lengthy and will not be presented here.

In Appendix A the elastic cross section was expressed in the form [Eq. (A24)]

$$\frac{d\sigma}{d\Omega} = \frac{q}{k} F^2(Q)[A + Bx + Cx^2]. \quad \text{(B8)}$$

The coefficients $A-C$ are defined in terms of the isovector amplitudes in Eq. (A25). We will designate them as $A^{(+)}$, $B^{(+)}$, and $C^{(+)}$ to distinguish them from coefficients constructed from the isoscalar amplitudes, designated respectively as $A^{(0)}$, etc. The quantity $x = \cos\theta$, where θ is the pion angle in the c.m. frame. From previous considerations we may also express the inelastic cross sections in terms of these coefficients. Including n-p partial waves up to $l=2$, we obtain

$$\left(\frac{d\sigma}{d\Omega}\right)_{T=0} = \frac{1}{2\pi^2 k} \int_0^{p_{\max}} qp^2 \left(f_0^2 + \frac{3}{2} f_1^2 + 5 f_2^2 \right) \times [A^{(+)} + B^{(+)} x + C^{(+)} x^2] dp,$$

$$\left(\frac{d\sigma}{d\Omega}\right)_{T=1} = \frac{1}{2\pi^2 k} \int_0^{p_{\max}} qp^2 \left(\frac{1}{2} f_0^2 + 3 f_1^2 + \frac{5}{2} f_2^2 \right) \times [A^{(0)} + B^{(0)} x + C^{(0)} x^2] dp, \quad \text{(B9)}$$

where the spin-dependence of $A-C$ is implicitly understood (e.g., P_3 is absent in singlet transitions).

The form factors $f_l(Q)$ appearing in Eq. (B9) are defined by Eq. (B6) in the plane-wave limit. The deuteron spatial wave function Ψ_d is given by the simple square-well model described in many textbooks. The well depth and radius are $V_i = 38.5$ MeV and $R_i = 1.93$ fm [24]. Our results are not very sensitive to these particular parameters since the cross sections are largely determined by the asymptotic behavior of the wave function, $\Psi_d \sim e^{-\gamma r}/r$, where $\gamma = 0.232$ fm^{-1} is fixed by the binding energy.

The plane-wave approximation for $f_l(Q)$ is adequate for n-p partial waves $l>0$, since the respective scattering phase shifts are small, but for S waves it is necessary to take into account the N-N final-state interaction. The final-state wave functions are evaluated in the square-well approximation, with parameters $V_f = 38.5$ MeV and $R_f = 1.93$ fm for the $^3S_1$ continuum and $V_f = 14.3$ MeV and $R_f = 2.50$ fm for the $^1S_0$ continuum [24]. Beyond the range R_f the continuum wave functions are given by

$$\Psi_f(l=0) \rightarrow \frac{e^{i\delta_0}}{pr} \sin(pr + \delta_0), \quad \text{(B10)}$$

where δ_0 is the S-wave phase shift. Note that this does not alter the basic formalism described by Eq. (B9); one merely replaces the Bessel function $j_0(pr)$ in Eq. (B6) by the appropriate distorted-wave function, asymptotically normalized to Eq. (B10). Since the S-wave form factor is now a complex quantity, it enters Eq. (B9) as $|f_0|^2$.

Finally, the S-wave phase shifts δ_0 are evaluated using the effective range approximation

$$p \cot \delta_0 = -\frac{1}{a_0} + \frac{1}{2} r_0 p^2, \quad \text{(B11)}$$

where the scattering length and effective range are, respectively, $a_0 = 5.4$ fm, $r_0 = 1.75$ fm for the triplet state and $a_0 = -24$ fm, $r_0 = 2.73$ fm for the singlet state [24]. The bound state and continuum parameters approximately satisfy the orthogonality requirement $\langle {}^3S_1 | {}^3S_1 \rangle = 0$.

The coefficients $A^{(i)}-C^{(i)}$ in Eq. (B9) are defined by Eq. (17) as derived from Eq. (A25), with $D=1$ since the D state is being ignored. The P-wave amplitudes are parametrized in terms of reduced amplitudes following the usual conjecture $P^{(+,0)}_{1,2,3}=p^{(+,0)}_{1,2,3}\cdot kq$ and $H^{(+,0)}_0=h^{(+,0)}_0\cdot kq$, where k and q are expressed in units of the pion mass. Most analyses agree that the isoscalar P-wave amplitudes are very small, and here we will adopt the ChPT predictions of Refs. [7,11,17]. Translated to our notation, the reduced amplitudes (in units of $10^{-3}/m_{\pi^+}$) are

$$p^{(0)}_1=1.5 \quad \text{and} \quad h^{(0)}_0=0.8. \tag{B12}$$

The effective isoscalar S-wave amplitude follows directly from the ChPT nucleon amplitudes of Eq. (3):

$$\overline{E}^{(0)}=-1.65. \tag{B13}$$

This should provide a reasonable estimate of the effective amplitude since, as elementary isospin considerations demonstrate, the two-nucleon rescattering corrections largely cancel in the isoscalar amplitude $E^{(0)}_{0+}$. The above roughly agrees with the ''old'' LET prediction $E^{(0)}_{0+}=-1.40$, not unexpected since the ChPT corrections from the ''triangle diagram'' cancel in the isoscalar amplitude.

The reduced isovector-even amplitudes as deduced from the ChPT results are $p^{(+)}_1=8.9$ and $h^{(+)}_0=7.8$. However, the present measurements are consistent with slightly larger amplitudes and we compromise with the values

$$p^{(+)}_1\approx 11 \quad \text{and} \quad h^{(+)}_0\approx 8.1. \tag{B14}$$

Actually, the total inelastic cross section as evaluated by explicit integration of $d\sigma/d\Omega$ is rather insensitive to $p^{(+)}_1$ (for a fixed $h^{(+)}_0$), as could be anticipated from the approximate elastic cross section of Eq. (A27).

The effective S-wave amplitude $\overline{E}^{(+)}$ is strongly influenced by the two-nucleon rescattering correction. The threshold amplitude deduced from the ChPT calculation [7] is given by Eq. (11), but in view of the present measurements we will adopt the slightly lower value

$$\overline{E}^{(+)}\approx -2.0, \tag{B15}$$

and in addition we will neglect any energy dependence such as might arise from unitarity and other considerations. In adopting Eq. (B15) we are assuming the rescattering correction is comparable for the elastic and inelastic channels, but this is not a crucial issue, since the transition to the $T=0$ continuum is dominated by the P-wave terms.

An error analysis of the input parameters suggests a theoretical uncertainty of about $\pm 25\%$ in the cross section. This uncertainty derives in large part from the isoscalar amplitude $\overline{E}^{(0)}$ [Eq. (B13)], to which we ascribe a nominal uncertainty of ± 0.3. The cross section is mildly dependent on the $^3S_1$ scattering length, but is quite insensitive to the $^1S_0$ scattering length.

We are unaware of any discussion in the literature with which we may compare the present calculation. As an alternative, we consider the related reaction $^2\mathrm{H}(\gamma,\pi^+)nn$ which has been calculated by Noble [25] using a rather different formalism than here. As applied to the charged pion channel, only the second ($T=1$) cross section of Eq. (B9) is relevant. The transformation to π^+ production introduces an extra factor of 1/2 in the cross section, and of course the appropriate $p(\gamma,\pi^+)$ multipoles enter the $A-C$ coefficients. For the S-wave multipole we adopt the usual Born value $E_{0+}(\pi^+ n)=28$, while the reduced P-wave amplitudes are given by $p_1=-2.0$ and $h_0=15.6$ [26], all in the usual units. Finally, the n-n scattering length is $a_0=-16.4$ fm, as in [25]. All other parameters are as previously specified.

The resulting total $^2\mathrm{H}(\gamma,\pi^+)nn$ cross section is in very good agreement with the cross section evaluated by Noble [25]. Both calculations fall about 10% below the experimental cross section of Booth *et al.* [27] (see Fig. 3 of Ref. [25] for a representative comparison of theory and experiment).

The same reaction was also measured by Audit *et al.* [28] with somewhat improved statistical precision, and the results are about 10% *lower* than reported by Booth *et al.* According to Ref. [28], the discrepancy has been resolved in favor of the lower cross section, which places the present calculation of $^2\mathrm{H}(\gamma,\pi^+)$ in excellent agreement with experiment and is an encouraging test of the formalism.

APPENDIX C: IMAGINARY PART OF $\overline{E}^{(+)}$

We present a simple estimate of the imaginary part of the effective amplitude $E^{(+)}$ and argue that it is negligible in the energy domain of the present experiment.

Generalizing Eq. (9) to include complex amplitudes in the region above threshold, we have the identity

$$\mathrm{Im}\ \overline{E}^{(+)}=\mathrm{Im}\ E^{(+)}_{0+}+\mathrm{Im}\ \Delta E, \tag{C1}$$

where

$$\mathrm{Im}\ E^{(+)}_{0+}=\frac{1}{2}\left[\mathrm{Im}\ E_{0+}(\pi^0 p)+\mathrm{Im}\ E_{0+}(\pi^0 n)\right] \tag{C2}$$

and ΔE is the two-nucleon rescattering contribution (below). The two terms in Eq. (C2) derive from one-nucleon rescattering and can be estimated from unitarity constraints using, for example, the conventional K-matrix formalism. For free nucleons one obtains

$$\begin{aligned}\mathrm{Im}\ E_{0+}(\pi^0 p)&=E_{0+}(\pi^+ n)a_{\mathrm{cx}}\overline{q},\\ \mathrm{Im}\ E_{0+}(\pi^0 n)&=-E_{0+}(\pi^- p)a_{\mathrm{cx}}\overline{q},\end{aligned} \tag{C3}$$

where $a_{\mathrm{cx}}=\sqrt{2}(a_1-a_3)/3$ is the $\pi^+ n\to\pi^0 p$ charge exchange amplitude and $\overline{q}$ is the on-shell momentum of the intermediate charged pion. The other S-wave multipoles describe $\gamma p\to\pi^+ n$ and $\gamma n\to\pi^- p$. Combining Eqs. (C2) and (C3), we obtain

$$\mathrm{Im}\ E^{(+)}_{0+}=\frac{1}{2}\ \eta[E_{0+}(\pi^+ n)-E_{0+}(\pi^- p)]a_{\mathrm{cx}}\overline{q}, \tag{C4}$$

where the factor η [Eq. (A7)] arises from the $\pi N\to\pi A$ frame transformation.

The two-nucleon rescattering contribution ΔE is given in the static approximation by [10]

$$\Delta E = -\frac{1}{2}\,\eta[E_{0+}(\pi^+ n) - E_{0+}(\pi^- p)]a_{\rm cx}\frac{\langle (1/r)e^{i\bar{q}\bar{r}}e^{i(\vec{\mathbf{k}}+\vec{\mathbf{q}})\cdot\vec{\mathbf{r}}/2}\rangle}{\langle e^{i(\vec{\mathbf{k}}-\vec{\mathbf{q}})\cdot\vec{\mathbf{r}}/2}\rangle}, \quad \text{(C5)}$$

where the expectation values are evaluated between deuteron states. To simplify the discussion we will neglect the D-state contribution, and from Eq. (C5) we then obtain

$$\text{Im}\,\Delta E = -\frac{1}{2}\,\eta[E_{0+}(\pi^+ n) - E_{0+}(\pi^- p)]a_{\rm cx}\frac{\langle (1/r)\sin\bar{q}r\, j_0(Q^+ r/2)\rangle}{\langle j_0(Q^- r/2)\rangle}, \quad \text{(C6)}$$

where $Q^{\pm} = |\vec{k} \pm \vec{q}|$.

Note that Im ΔE as defined by Eq. (C6) is a *negative* quantity. However, unitarity demands that the physical amplitude Im $\bar{E}^{(+)}$ be positive definite, and so some additional compensating term must be present, and of course this is precisely the one-nucleon rescattering term Im $E_{0+}^{(+)}$. The point is that a consistent treatment of Im $\bar{E}^{(+)}$ requires that *both* rescattering contributions be evaluated within a single common framework, as opposed to treating them as mutually independent processes.

Consider now the expansion of Eq. (C6) in terms of the generic pion momenta $(q,\bar{q})$. To lowest order we find

$$\text{Im}\,\Delta E = -\frac{1}{2}\,\eta[E_{0+}(\pi^+ n) - E_{0+}(\pi^- p)]a_{\rm cx}\bar{q}, \quad \text{(C7)}$$

which exactly cancels the contribution expressed by Eq. (C4). We thus reach the remarkable conclusion that the free-nucleon imaginary amplitudes, Eq. (C3), which are substantial even at low energy, are not a deciding factor in the strength of Im $\bar{E}^{(+)}$. Indeed, in our simplified scheme the strength of Im $\bar{E}^{(+)}$ is mainly decided by terms of order $\bar{q}^3$, which are demonstrably much smaller than the imaginary parts of the free-nucleon amplitudes. These conclusions are confirmed by explicit numerical evaluation of Eq. (C6). Since Im $\bar{E}^{(+)}$ enters the differential cross section in quadratic form (there are no interference terms), little loss in generality results from setting Im $\bar{E}^{(+)}=0$ in the analysis of Sec. IV.

We expect that the leading-order cancellation will still prevail in a more refined calculation; for example, one which properly incorporates Fermi motion. Indeed, preliminary results from such a comprehensive calculation [26] support our conclusion that Im $\bar{E}^{(+)}$ is negligible over the present energy domain.

[1] P. Argan *et al.*, Phys. Lett. B **206**, 4 (1988).
[2] M. Fuchs *et al.*, Phys. Lett. B **368**, 20 (1996).
[3] J. C. Bergstrom, R. Igarashi, and J. M. Vogt, Phys. Rev. C **55**, 2016 (1997); See also J. C. Bergstrom, J. M. Vogt, R. Igarashi, K. J. Keeter, E. L. Hallin, G. A. Retzlaff, D. M. Skopik, and E. C. Booth, *ibid.* **53**, R1052 (1996); J. C. Bergstrom, *πN Newsletter*, edited by D. Drechsel, G. Höhler, W. Kluge, B. M. K. Nefkens, and H.-M. Staudenmaier (Universität Karlsruhe, Germany, 1997), Vol. 12, p. 1.
[4] A. M. Bernstein, E. Shuster, R. Beck, M. Fuchs, B. Krusche, H. Merkel, and H. Ströher, Phys. Rev. C **55**, 1509 (1997).
[5] J. H. Koch and R. M. Woloshyn, Phys. Rev. C **16**, 1968 (1977).
[6] F. Blaazer, B. L. G. Bakker, and H. J. Boersma, Nucl. Phys. **A590**, 750 (1995).
[7] S. R. Beane, V. Bernard, T.-S. H. Lee, Ulf-G. Meissner, and U. van Kolck, Nucl. Phys. **A618**, 381 (1997).
[8] T. Ericson and W. Weise, *Pions and Nuclei* (Clarendon, Oxford, 1988).
[9] P. Bosted and J. M. Laget, Nucl. Phys. **A296**, 413 (1978).
[10] S. S. Kamalov, L. Tiator, and C. Bennhold, Phys. Rev. C **55**, 98 (1997). The second term in their Eq. (27) has the wrong sign.
[11] V. Bernard, N. Kaiser, and Ulf-G. Meissner, Z. Phys. C **70**, 483 (1996).
[12] J. M. Vogt, R. E. Pywell, D. M. Skopik, E. L. Hallin, J. C. Bergstrom, and H. S. Caplan, Nucl. Instrum. Methods Phys. Res. A **324**, 198 (1993).
[13] J. M. Vogt, J. C. Bergstrom, R. Igarashi, and K. J. Keeter, Nucl. Instrum. Methods Phys. Res. A **366**, 100 (1995).
[14] J. C. Bergstrom, R. Igarashi, and J. M. Vogt, Phys. Rev. C **55**, 2923 (1997).
[15] P. R. Bevington, *Data Reduction and Error Analysis for the Physical Sciences* (McGraw-Hill, New York, 1969).
[16] J. C. Bergstrom, Phys. Rev. C **50**, 2979 (1994).
[17] V. Bernard, N. Kaiser, and Ulf-G. Meissner, Phys. Lett. B **378**, 337 (1996).
[18] P. Wilhelm and H. Arenhövel, Nucl. Phys. **A593**, 435 (1995).
[19] O. Hanstein, D. Drechsel, and L. Tiator, Phys. Lett. B **399**, 13 (1997).
[20] P. Wilhelm, Phys. Rev. C **56**, R1215 (1997).
[21] L. Tiator and L. E. Wright, Phys. Rev. C **30**, 989 (1984).
[22] C. Lazard, R. J. Lombard, and Z. Maric, Nucl. Phys. **A271**, 317 (1976).
[23] G. G. Simon, Ch. Schmitt, and V. H. Walther, Nucl. Phys. **A364**, 285 (1981).
[24] W. E. Burcham, *Elements of Nuclear Physics* (Longman, New York, 1979).
[25] J. V. Noble, Phys. Lett. **67B**, 39 (1977).
[26] M. Benmerrouche (private communication).
[27] E. C. Booth, B. Chasan, A. M. Bernstein, P. Bosted, and J. H. Koch, Phys. Lett. **66B**, 236 (1977).
[28] G. Audit *et al.*, Phys. Rev. C **16**, 1517 (1977).